1 November 1999

ELSEVIER

Optics Communications 170 (1999) 291–297

OPTICS COMMUNICATIONS

www.elsevier.com/locate/optcom

Self-bending of photorefractive solitons

J. Petter [a,*], C. Weilnau [a], C. Denz [a], A. Stepken [b,1], F. Kaiser [b]

[a] *Light- and Particle Optics, Institute of Applied Physics, Darmstadt University of Technology, Hochschulstr. 6, D-64289 Darmstadt, Germany*

[b] *Theoretical Nonlinear Dynamics, Institute of Applied Physics, Darmstadt University of Technology, Hochschulstr. 4, D-64289 Darmstadt, Germany*

Received 9 June 1999; received in revised form 1 September 1999; accepted 2 September 1999

Abstract

Self-bending of photorefractive solitons is caused by diffusion in photorefractive crystals and becomes an important effect when the beam size is in the range of the charge carriers diffusion length. In this paper we present an experimental and numerical examination of the beam bending dependence on relevant parameters such as the applied electric field and the beam intensity. We demonstrate that the bending dependence on the electric field in the low saturation regime has the form of a square function at low values of the field and becomes linear for higher values. For stronger saturation the curve gets the form of a square root function. The bending dependence on the beam intensity has a maximum at defined intensity. The experimental data are compared with numerical simulations, giving a good qualitative agreement.

PACS: 42.65.Tg; 42.65.Wi; 42.79.Gn
Keywords: Soliton; Bending; Photorefractive

1. Introduction

Optical spatial screening solitons in photorefractive materials have found a growing interest in the last decade [1]. Due to their feature of formation at very low laser power and their robust character they are easy to achieve and therefore very promising for applications, e.g. adaptive waveguiding or all optical switching [2]. While the structure and the anomalous interaction between photorefractive screening (steady state) solitons have been studied extensively (e.g. [3,4]), we focus our examination on the effect of the lateral shift of the beam, known as beam bending, and its dependence on the applied electric field and the beam intensity.

A soliton in a photorefractive crystal forms when self-focusing inside the nonlinear material exactly balances the diffraction of the propagating light beam. Charge carriers are excited in the illuminated regions of the crystal. Subsequently the charges move to darker regions caused by drift- and diffusion transport mechanisms, and lead to a space charge field inside the crystal. Due to the electro-optic effect this field leads in turn to a refractive index modulation in form of a focusing lens. Therefore the light beam effectively traps itself in a self-written waveguide

* Corresponding author. E-mail: juergen.petter@physik.tu-darmstadt.de
[1] E-mail: andreas.stepken@physik.tu-darmstadt.de

0030-4018/99/$ - see front matter
PII: S0030-4018(99)00485-X

[5]. Because of the high gradient of the light intensity between the focused beam and dark regions of the crystal, diffusion of photoexcited charge carriers in the material becomes dominant [6]. This leads to a deformation of the induced lens in the direction of the applied field which shifts the beam in the same direction. As a result, the trajectory of the soliton inside the crystal is bent [7,8]. Depending on the chosen parameters the bending distance at the exit face of the crystal can reach several beam diameters. Previous numerical simulations showed that the trajectory of a steady state soliton follows a parabolic curve [7–9]. In this experiment however, the observation of the soliton is limited to the beam position at the exit face of the crystal. Due to the scattering of light inside the crystal the side-view imaging of the soliton trajectory is not possible [10]. To achieve control of this bending, which is necessary to realize e.g. beam guiding and beam switching, exact knowledge of the dependence on the applied electric field and the intensity ratio is indispensable. The aim of this paper is the examination of these dependencies in experimental and in numerical simulations.

2. Experiment

The experimental examination of beam bending is realized in a standard setup shown in Fig. 1. The beam of a frequency-doubled Nd:YAG laser ($\lambda = 532$ nm) is focused to a size of nearly 10 μm onto the front face of a SBN (Strontium Barium Niobat) crystal, biased with an electric field (0–3 kV) in direction of its crystallographic c-axis. The dimensions of the crystal are $5 \times 5 \times 13.5$ mm with the c-axis along one 5 mm side and the propagation direction along the 13.5 mm side. To make use of the dominant electro-optic coefficient r_{33} of the SBN-crystal, the polarization of the beam is chosen to be parallel to the direction of the crystal's c-axis. The bending distance at the back face of the crystal is monitored with a CCD-camera.

The photorefractive nonlinearity has a saturable character. The process of screening of the external field is therefore determined by the degree of saturation, which is defined as the ratio between the soliton peak intensity and the background illumination. To control the saturation level, the crystal is illuminated with a wide beam provided from an incoherent white light source. The intensity of the background illumination was measured indirectly with two-beam coupling experiments where the coupling constant γ depends on the background illumination [11]. However this measurement includes a large uncertainty leading to an inaccuracy of $\approx 20\%$ in the determination of the background illumination.

3. Soliton formation

Fig. 2 shows a typical scenario of a soliton formation and its related bending in experiment. Without

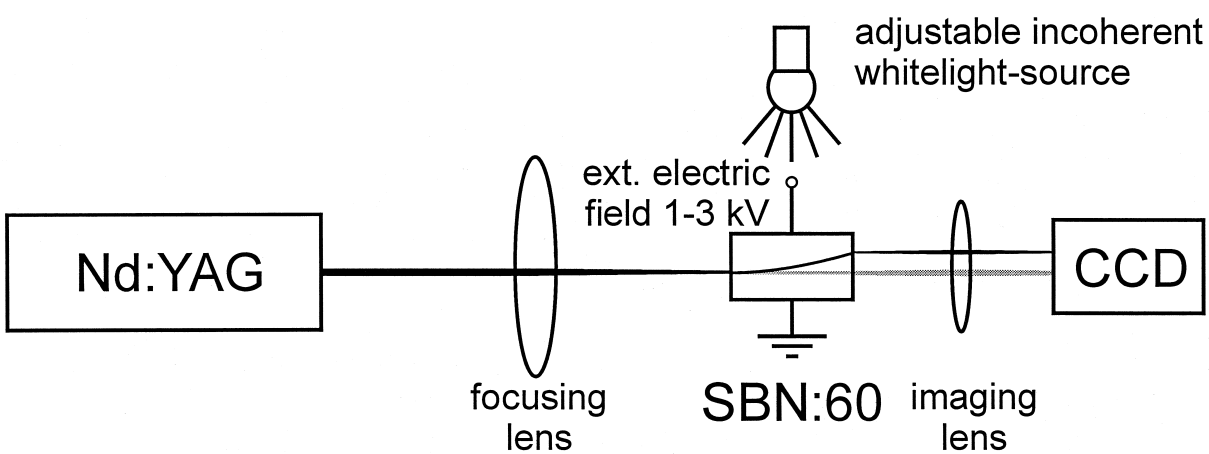

Fig. 1. Setup for formation of photorefractive solitons.

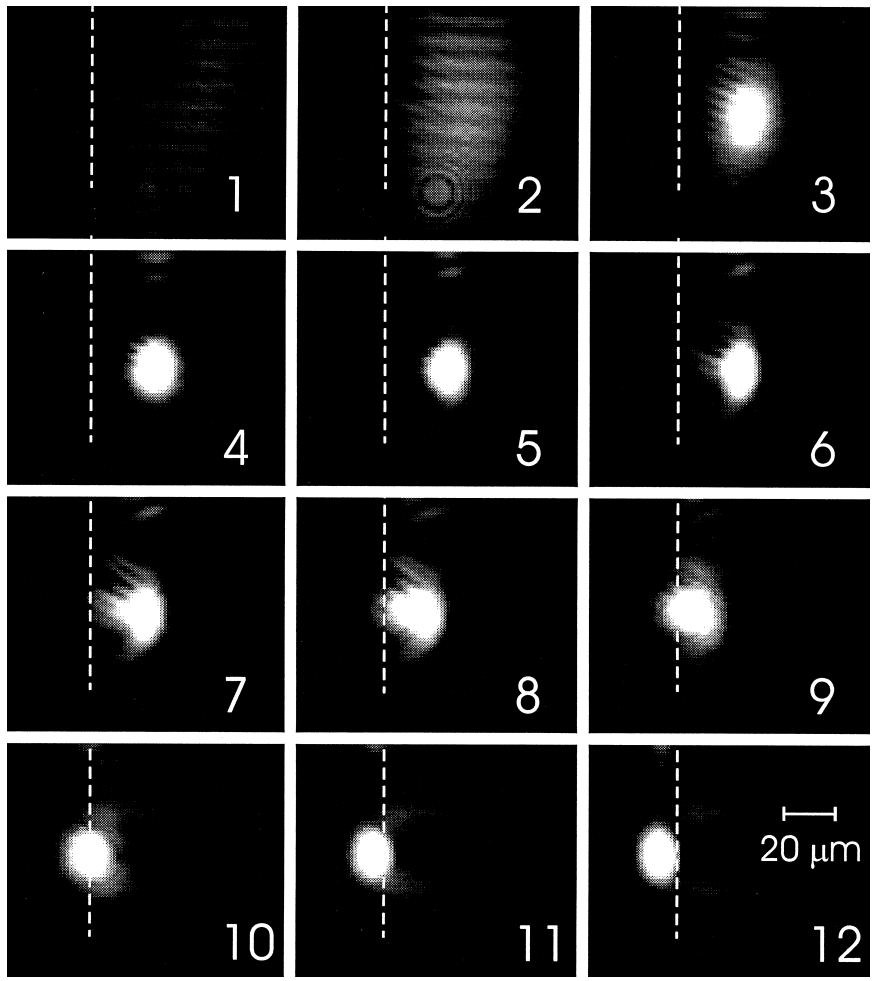

Fig. 2. Formation and dynamics of a soliton as seen at the exit face of the crystal. The sequence starts 0.2 s after the external field is switched on and the time interval between consecutive snapshots is 0.2 s. The external electric field points to the left.

applying an electric field, the diameter of the beam with an intensity of 6 μW reaches a size of > 100 μm after propagating through the crystal. When applying the electric field (4,6 kV/cm) the beam starts to focus within the next 0.8 s to a size of ≈ 10 μm due to the drift of the charge carriers and the resulting space-charge field inside the crystal (see Fig. 2,1–4). As focusing proceeds the peak intensity of the soliton rises and the diffusion of the charge carriers becomes a more important effect. This leads to bending of the beam trajectory, in agreement with [7]. In the same time interval the beam experiences transient oscillations in its diameter which may result for a short period of time in almost a doubling of the former beam diameter. After a typical time, depending on the crystals relaxation time and the applied electric field, the effect reaches a steady state when the space-charge field compensates for the biased electric field. In the situation shown in Fig. 2,12 the steady state is reached 2.4 s after switching on the electric field. It should be noted that the soliton has an elliptical shape after its first focusing (Fig. 2,6) and again in steady state. The diameter-ratio is ≈ 1.5 in agreement to previous examinations [11]. The same behaviour can be found in numerical simulations shown in Fig. 3. The calculations are based on

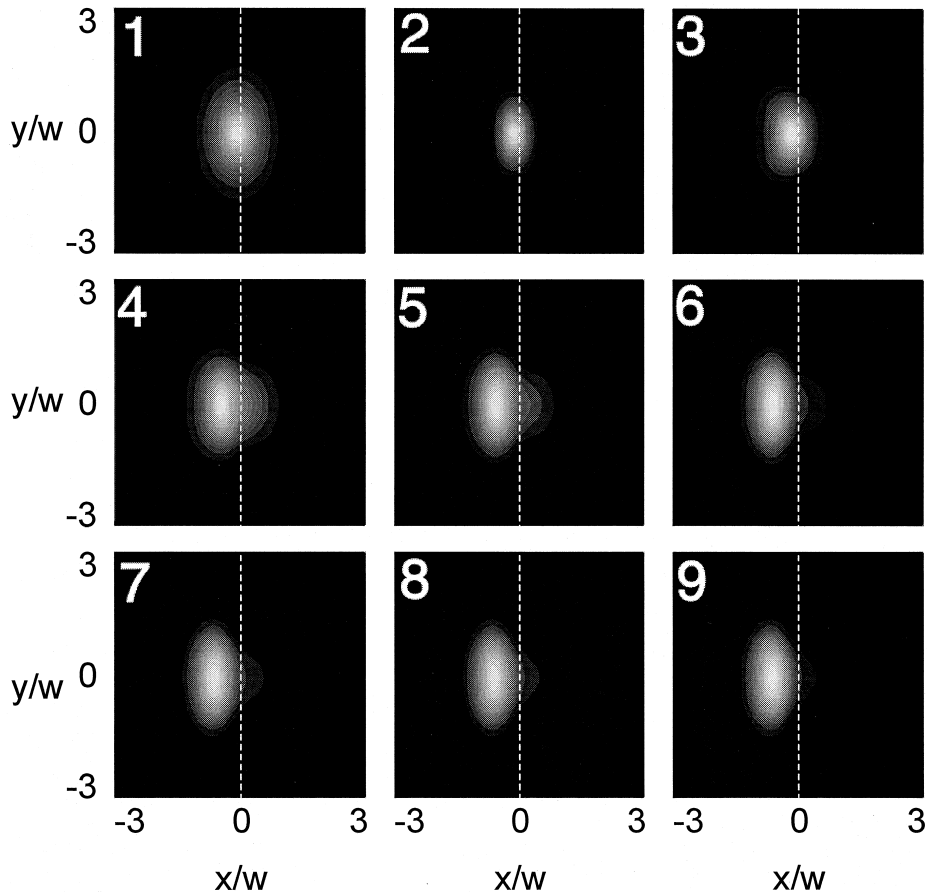

Fig. 3. Numerical simulation of soliton development and bending.

the equations given in Section 5 of this paper. Shortly after the gaussian beam is launched into the crystal biased with an electric field (4.5 kV/cm) it starts to focus to an elliptical shaped spot with a diameter of 7 μm in x- and 14 μm in y-direction. Because computing time for simulations rises considerably with propagation length, it was chosen to 3.4 mm, since the same qualitatively behaviour can be seen. After 1.8 τ, where τ is the characteristic relaxation time of the crystal, the strongly focused beam breaks up and starts to shift in the direction of the applied field while its diameter almost doubles in both directions. Within the next 5.4 τ the beam moves about the length of 1/2 of the beam diameter into the direction of the applied electric field where it reaches steady state 7.2 τ after launching. In comparison to the experimental data the shorter bending distance can be explained due to the shorter propagation length. Note in Fig. 3,4–7 the hump at the right side of the beam which is left at the former beam position while bending. This hump has its origin in the refractive index change which slowly is erased by the background illumination.

4. Dependence on the electric field

In changing major parameters of the experiment, as the value of the electric field or the intensity of the beam, one can easily control the bending in its spatial and temporal development. In Fig. 4 the bending distance at the exit face of the crystal is plotted in dependence on the applied electric field. In this measurement the intensity of the laser beam

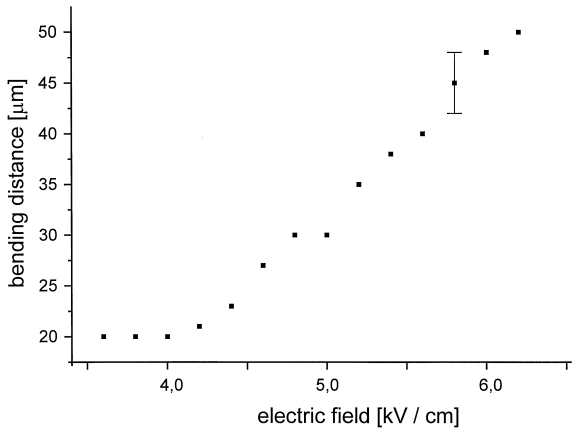

Fig. 4. Dependence of beam bending on the applied electric field.

launched into the crystal was fixed at 8.1 μW with an initial diameter of ≈ 17 μm and the intensity ratio between the beam and background illumination ($I_{\mathrm{Beam}}/I_{\mathrm{Back}}$) was set to ≈ 1.

Under these conditions a soliton forms at an externally applied electric field of 1.8 kV (3.6 kV/cm). When increasing the electric field to 3.0 kV (6.0 kV/cm) the bending distance rises to 45 μm, which is more than 2.5 times the diameter of the beam. When we rise the electric field above 3.0 kV strong dynamics and turbulence starts and therefore no stable position of the soliton can be found. In this region the stability of the soliton solution is no longer present, leading to filamentation dynamics [10].

5. Numerical methods

The behaviour of screening solitons in photorefractive media can be described by the standard wave equation in paraxial approximation and the Kukhtarev material equations [12]. The propagation equation has the following form

$$\left[\frac{\partial}{\partial z} + \boldsymbol{\Theta}\cdot\nabla - \frac{i}{2}\nabla^2\right]A = \frac{i\gamma}{2}\left(\frac{\partial\varphi}{\partial x} - E_0\right)A, \qquad (1)$$

for the slowly-varying envelope of the beam $A(\boldsymbol{r})$. The vector $\boldsymbol{\Theta}$ specifies the direction of beam launching, ∇ is the transverse gradient, and $\gamma = k^2 n^4 w^2 r_{\mathrm{eff}}$ is the medium-light coupling constant. Here k is the wave number of light in the vacuum, n is the unperturbed index of refraction, w is the initial beam spot size, and r_{eff} is the effective element of the electro-optic tensor. The transverse coordinates x and y are scaled by w and the propagation direction z is scaled by the diffraction length $L_{\mathrm{D}} = knw^2$.

φ is the electrostatic potential induced by the light, whose evolution is governed by the following relaxation equation

$$\tau\frac{\partial}{\partial t}\left(\nabla^2\varphi\right) + \nabla^2\varphi + \nabla\varphi\cdot\nabla\ln I = E_0\frac{\partial}{\partial x}\ln I + \frac{k_{\mathrm{B}}T}{e}\left[\nabla^2\ln I + (\nabla\ln I)^2\right], \qquad (2)$$

where τ is the relaxation time of the crystal and E_0 is the external field. The total intensity $I = 1 + |A|^2$ is measured in units of the saturation intensity. The terms on the right side of Eq. (2) describe the effect of drift and diffusion of charges in the crystal.

Eqs. (1) and (2) are integrated numerically for a range of initial conditions. All parameters correspond to the experimental situation introduced above. Since the response of the SBN crystal is rather slow (τ is of the order of seconds), the dynamics of beam is slaved to the crystal. All temporal changes stem from the potential equation [13]. Fig. 5 shows the bending distance in dependence on the external field for two different normalized intensities from numerical simu-

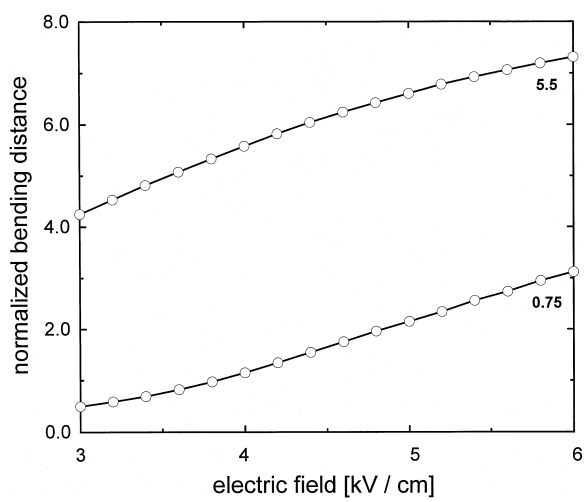

Fig. 5. Numerical simulation of the dependence of the bending distance on the applied electric field for two different normalized intensities: lower plot $I = 0.75$, upper plot $I = 5.5$. The bending distance is normalized to the beam diameter.

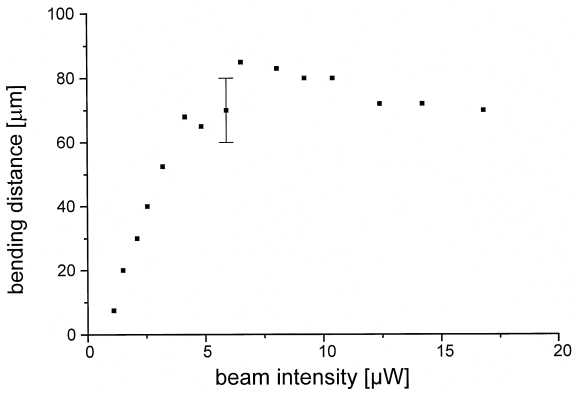

Fig. 6. Dependence of beam bending on the beam intensity.

lations. In both cases the beam has an initial diameter of 12 μm and propagates for 13.5 mm. The normalized intensity in the lower plot was set to 0.75, in the upper plot to 5.5.

Comparing the numerical simulation to the experimentally found data we can see a good qualitative agreement for the range of low saturation. As shown in the upper plot in Fig. 5 in the range of higher saturation ($I_{\mathrm{Beam}}/I_{\mathrm{Back}} > 1$), the form of the curve changes from a quadratic relation to a curve with square root characteristic. Therefore the analysis of the curve can be a useful tool for determination of the value of saturation. The reason of this change is presently under investigation.

6. Dependence on intensity ratio

Fig. 6 shows the results of the experimental examination of the bending distance in dependence on the beam intensity. Here the value of the external electric field was fixed at 2.7 kV (5.4 kV/cm). The intensity of the beam was adjusted to be in the range of 1 μW up to 17 μW while the diameter of the initial beam was 12 μm.

In the low saturation regime ($1 > I_{\mathrm{Beam}}/I_{\mathrm{Back}}$), the bending of the soliton increases strongly with increasing beam intensity. On further increase of the intensity the slope of the bending curve slowly decreases until it reaches a maximum at a beam intensity of 6 μW. In the regime of higher saturation the bending distance slowly decreases with increasing intensity.

Fig. 7 shows a numerical simulation of the dependence of the beam bending distance on the normalized intensity. The external field was set to 5 kV/cm and the propagation length was 12.5 mm. Comparing these data with those found experimentally we can see a good qualitative agreement. The decrease of the bending distance at higher beam intensities is mainly due to the beam widening and the therefore smaller gradient for the saturated nonlinearity. The difference between experimental data and numerical simulation can be explained due to absorption losses, neglected in the numerical simulations.

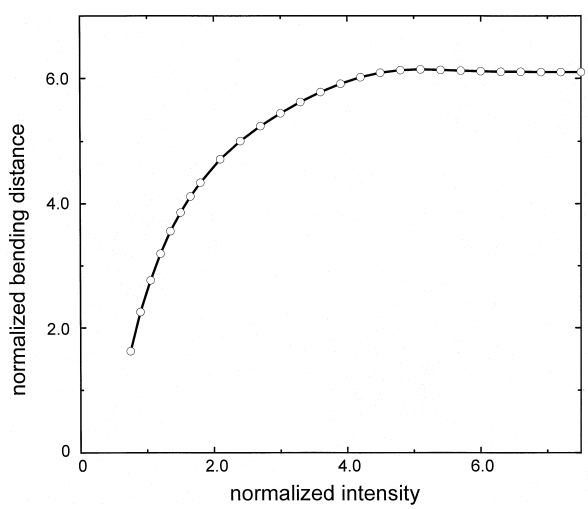

Fig. 7. Numerical simulation of the dependence of the bending distance on the normalized intensity.

The characteristic dependence of the bending distance on the intensity can be explained due to the diameter of the beam. As shown in [11], the diameter of the soliton decreases in the low saturation regime with increasing intensity. At a normalized intensity of ≈ 4 the diameter of the soliton becomes minimal. With further increase of the intensity the beam slowly widens again since no more charge carriers can be excited in the central region of the beam. For smaller beams their diameter is in the range of the diffusion length of the charge carriers, thus diffusion becomes dominant and the bending increases. When the diameter of the beam reaches its minimum, the bending distance reaches a maximum and slowly decreases with increasing intensity.

Another method to examine the dependence of bending on the intensity is given in [14] where the electric field was adjusted for every different intensity ratio to maintain a circular soliton solution. In this case linear dependence of beam bending for high values of intensity was found.

7. Conclusion

The precise control of the beam bending in photorefractive crystals is an interesting possibility to realize adaptive beam guiding and all optical switches. We have shown that the bending distance follows a well-defined dependence on the applied electric field and the intensity and thus provides easy control parameter. In our experiments we were able to vary the bending distance in the range of 25 μm in rising the applied electric field from 1.8 kV–3.0 kV. Another control parameter of the bending distance is the intensity ratio between the beam and the background illumination. After a strong increase of the bending distance with increasing beam intensity in the low saturation regime, the bending reaches a maximum at an intensity of 6 μW and slowly decreases on further increase of the beam intensity. This dependence can be explained by the changing diameter of the soliton, which decreases with increasing intensity and reaches a minimum at a normalized intensity of ≈ 4.

Acknowledgements

This research was partially supported by the Deutsche Forschungsgemeinschaft under contract KA-708/1-1. The authors would like to acknowledge helpful discussions with Dr. W. Krolikowski, Australian National University, Canberra and support by Prof. T. Tschudi, Institute of Light- and Particle Optics, Darmstadt University of Technology.

References

[1] M. Segev, Opt. Quant. Electr. 30 (1998) 503.
[2] M. Morin, G. Duree, G. Salamo, M. Segev, Opt. Lett. 20 (1995) 2066.
[3] H. Meng, G. Salamo, M. Segev, Opt. Lett. 23 (1998) 897.
[4] W. Krolikowski, M. Saffman, B. Luther-Davies, C. Denz, Phys. Rev. Lett. 80 (1998) 3240.
[5] N.V. Kukhtarev, V.B. Markov, S.G. Odulov, M.S. Soskin, V.L. Vinetskii, Ferroelectrics 22 (1979) 961.
[6] J. Feinberg, J. Opt. Soc. Am. 72 (1982) 46.
[7] W. Krolikowski, N. Akhmediev, B. Luther-Davies, M. Cronin-Golomb, Phys. Rev. E 54 (1996) 5761.
[8] S.R. Singh, M.I. Carvalho, D.N. Christodoulides, Opt. Commun. 130 (1996) 288.
[9] S. Gatz, J. Hermann, Opt. Lett. 23 (1998) 1176.
[10] A.A. Zozulya, D.Z. Anderson, A.V. Mamaev, M. Saffman, Phys. Rev. A 57 (1998) 522.
[11] A.A. Zozulya, D.Z. Anderson, A.V. Mamaev, M. Saffman, Europhys. Lett. 36 (1996) 419.
[12] A.A. Zozulya, D.Z. Anderson, Phys. Rev. A 51 (1995) 1520.
[13] A. Stepken, M.R. Belic, F. Kaiser, W. Krolikowski, B. Luther-Davies, Phys. Rev. Lett. 82 (1999) 540.
[14] M. Shih, P. Leach, M. Segev, M. Garrett, G. Salamo, G. Valley, Opt. Lett. 21 (1996) 324.